Supplementary Information

An acid microenvironment-driven theranostics platform for lung cancer ^{19}F MR/PA/FL multimodal imaging-guided photothermal therapy

Maosong Qiu, Lei Zhang, Yu Li, Ruifang Wang, Long Xiao, Shizhen Chen*, Xin Zhou*

Key Laboratory of Magnetic Resonance in Biological Systems, State Key Laboratory of Magnetic Resonance and Atomic and Molecular Physics, National Center for Magnetic Resonance in Wuhan, Wuhan Institute of Physics and Mathematics, Innovation Academy for Precision Measurement Science and Technology, Chinese Academy of Sciences; Wuhan National Laboratory for Optoelectronics, Huazhong University of Science and Technology (HUST), Wuhan 430071, China.

* Corresponding authors

E-mail addresses: chenshizhen@wipm.ac.cn (S. Chen), xinzhou@wipm.ac.cn (X. Zhou).

Table of Contents

Chemicals and reagents

Unless otherwise specified, all chemicals were of analytical grade that could be used directly without further purification. Gold (III) chloride trihydrate ($HAuCl_4 \cdot 3H_2O$), cetyltrimethylammonium bromide (CTAB), silver nitrate ($AgNO_3$), ascorbic acid (AA), sodium borohydride ($NaBH_4$), concentrated sulfuric acid (H_2SO_4), and new indocyanine green (IR820) were bought from Aladdin Reagent (Shanghai, China). Zinc nitrate hexahydrate ($Zn(NO_3)_2 \cdot 6H_2O$), 2-methylimidazole (2-MIM), trifluoromethylimidazole (TFMIM), polyvinylpyrrolidone (PVP, K30), and methanol were purchased from Shanghai Macklin Biochemical Co., Ltd. Pluronic F127 (F127), new indocyanine green (IR820), and fluorescein isothiocyanate (FITC) were ordered from Sigma-Aldrich (MO, USA). Deionized water (18.2 MΩ·cm) used in all experiments was purified with a Milli-Q Academic water purification system (Millipore Milli-Q grade).

Characterization of the nanoparticles

The transmission electron microscope (FEI Company, USA) and a ZS nanohybrid analyzer (Malvern, England) were used for the characterization of nanoparticles. The element distribution of nanoparticles was assessed by the HAADF-STEM (Oxford x-met 8000). The absorption spectra of the different samples were recorded by using an ultraviolet-visible-near infrared (UV-Vis-NIR) spectrophotometer (Thermo Fisher Scientific Inc., USA). The element analysis was performed by XPS (ESCA Lab 250, Thermo Fisher Scientific, USA) experiments. Crystalline structures are analyzed by X-ray diffraction (XRD) on a D8 Focus diffractometer (Bruker, Germany). The gold

concentration of the samples was measured by ICP-OES (Agilent 5110, USA). All *in vitro* and *in vivo* ^{1}H and ^{19}F MRI experiments were performed on a 9.4 T micro-imaging system (Bruker Avance 400, Ettlingen, Germany).

Synthesis of gold nanorods

The synthesis of gold nanorods (GNRs) was performed according to the classical seed-mediated growth method as described below [1]. Firstly, the seed solution was manufactured by adding 0.6 mL of cold $NaBH_4$ (0.01 M) into a mixture solution composed of 5 mL $HAuCl_4$ (0.5 M) and 1.5 mL CTAB (0.2 M). The solution was stirred vigorously for 3 min, and the color of the mixed solution turned from yellow to brownish-yellow. Secondly, the growth solution was synthesized as follows: 200 mL of CTAB (0.1 M), 2.0 mL $AgNO_3$ (0.01 M), and 10 mL of $HAuCl_4$ (0.01 M) were lightly mixed at 30 °C. Next, 1.6 mL of AA (0.1 M) was added to the solution to reduce gold from Au^{3+} to Au^{1+}. The color of the solution turned from yellow to colorless in a few seconds. At this point, 4 mL of H_2SO_4 (0.55 M) solution was added. After 30 min, 0.5 mL of seed solution was added to the entire growth solution, and the mixture was left undisturbed at 30 °C for 12 h. The obtained solution was centrifuged at 10,000 rpm for 10 min to remove additional CTAB and stored in 40 mL ultrapure water for future use.

Photothermal performance of nanoparticles

The GFZ PBS solutions at various concentrations (1 mL) were exposed to an 808 nm NIR laser (1 W/cm^2) for 400 seconds, respectively. Another experiment was

performed using a 12.5 μg/mL (C_{Au}) GFZ PBS solution (1 mL) that was illuminated by various power densities of the NIR laser (808 nm, 1 W/cm^2). Moreover, 12.5 μg/mL (C_{Au}) of GFZ PBS solution (1 mL) was irradiated by 808 nm laser (1 W/cm^2) for five cycles to evaluate its photothermal stability. The photothermal conversion efficiency of GFZ was determined by our previous method [2]. For the photothermal synergistic enhancement experiment of GFZI, the temperature change of IR820, GFZ, and GFZI was monitored after irradiation for 400 seconds. A laser energy meter (Coherent Inc., CA, USA) was used to determine the NIR laser power density. The real-time temperatures of the solutions were recorded using an infrared thermal imaging system.

Cell culture

The A549 cells and MRC-5 cells were obtained from the cell bank of Chinese Academy of Sciences (Shanghai, China) and cultured in DMEM supplemented with 10% heat-inactivated fetal bovine serum, 100 U/mL penicillin, and 100 μg/mL streptomycin under a humidified air with 5% CO_2 at 37 °C. All agents were purchased from Boster (Wuhan, China) and filtered with a 0.2 μm sterile filter before incubation with cells.

Cellular uptake of GFZF

A549 cells were incubated with GFZF (12 μg/mL) at different times (0.5 h, 2 h, 6 h, and 12 h), and stained with DAPI for 4 min. After that, the fluorescence intensity of treated cells was determined by confocal microscopy. Next, the uptake efficiency of

GFZF between A549 cells and MRC-5 cells was assessed by a confocal laser scanning fluorescence microscope (CLSM) (A1R/A1, Nikon, Japan) imaging after incubation with GFZF for 6 h. Besides, the flow cytometry (Beckman Coulter) was applied to the quantity of cellular fluorescence intensity.

Multicellular spheroids preparation and tumor penetration assay

To generate multicellular spheroids (MCSs), LLC cells were cultured using ultra-low attachment plates for about 3 days [3]. Next, MCSs were cultured in DMEM with different pH values, followed by treatment with the GFZF nanoparticles (12 μg/mL) for 2 h. The resultant MSCs were washed by PBS, re-suspended in a fresh medium, and subsequently detected by CLSM.

Cytotoxicity assessment

The cytotoxicity of GFZI on A549 cells and MRC-5 cells was evaluated by the CCK8 assay, respectively. The A549 cells and MRC-5 cells were seeded in 96-well culture plates at a density of approximately 1×10^4 cells per well and incubated for 24 h. The GFZI solution was diluted to 6, 12, 25, 50, 100, and 200 μg/mL using DMEM and added to the 96-palate wells. Cells cultured with DMEM were used as a control. After incubating for 4 h at 37 °C, the media was removed and the 200 μL of DMEM containing 20 μL CCK8 was added to the wells, and cells were incubated for 2 h at 37 °C. Finally, the optical density at 450 nm of each well was recorded on the ELISA plate reader (Spectra MAX 190, Molecular Devices). The cell viability of control

groups was assessed as the percentages of viable cells. All data are presented as mean ± SD, n > 3.

GFZI-mediated photothermal therapy *in vitro*

Firstly, the photothermal toxicity of GFZI was evaluated by the CCK8 method. After incubation with different concentrations of GFZI, the A549 cells and MRC-5 cells were irradiated with 808 nm laser (1 W/cm^2) for 10 min, respectively. Next, the cell viability was measured by the standard CCK8 method. For the confocal fluorescence imaging and flow cytometric assay, A549 cells were incubated with PBS or GFZI for 6 h. Then, the cells were washed with PBS three times and irradiated with an 808 nm laser for 10 min or not. After that, the cells were stained with Calcein AM/PI to visualize living cells (green) and dead cells (red) and imaged by CLSM. Moreover, the cells were collected and stained by Annexin V-FITC/PI for 15 min and analyzed by flow cytometry (Beckman Coulter).

Hemolysis assay

According to our previous work [2], the red blood cells (RBCs) were obtained from BALB/c mice and incubated with various concentrations of GFZI at 37ºC for 2 h. Then the samples were centrifuged and the supernatant was added into a 96-well chamber. Finally, the absorbance of the supernatant was measured at 541 nm using the ELISA plate reader (Spectra MAX 190, Molecular Devices). RBCs incubated with deionized water and PBS were used as the positive and negative controls, respectively. Finally, the hemolysis percentage values were calculated via the formula: Hemolysis (%) = $(A_s - A_n)/(A_p - A_n)$, where the A_s represented the sample absorbance, A_p represented the positive control absorbance, and A_n represented the negative

control absorbance. The experiment for each sample was repeated three times.

Animal and tumor model

Balb/c male nude mice (5 weeks of age, approximately 20 g) were obtained from Beijing Vital River Laboratory Animal Technology Co., Ltd. All experimental protocols in this study were approved by Animal Care and Use Committees at the Innovation Academy for Precision Measurement Science and Technology, the Chinese Academy of Sciences. To establish the subcutaneous A549 tumor-bearing mice model, 100 μL of A549 cells (5×10^7 cells/mL) were subcutaneously injected into the leg [4]. After four weeks, the tumor-bearing mice could be used for *in vivo* experiments.

Statistical analysis

All the data are presented as mean ± SD. Experiments were performed in triplicate unless otherwise stated. A one-way analysis of variance was used to determine the significance of the difference. (*$p < 0.05$, **$p < 0.01$, ***$p < 0.001$).

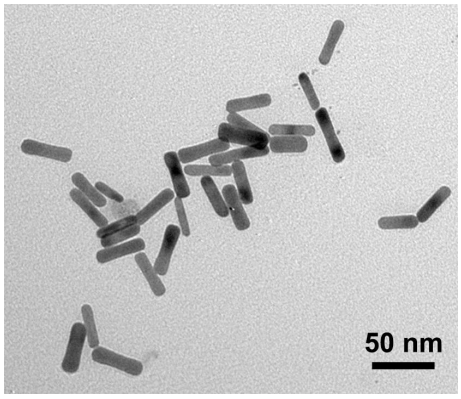

Figure S1. TEM image of GNRs.

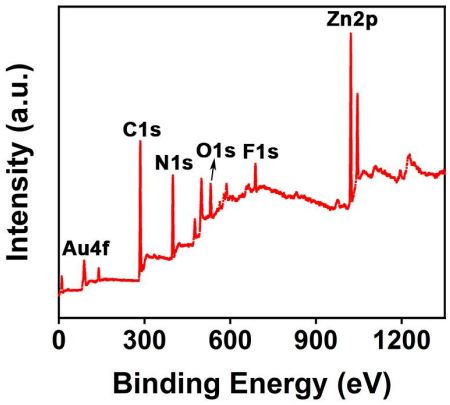

Figure S2. XPS spectra of GFZ.

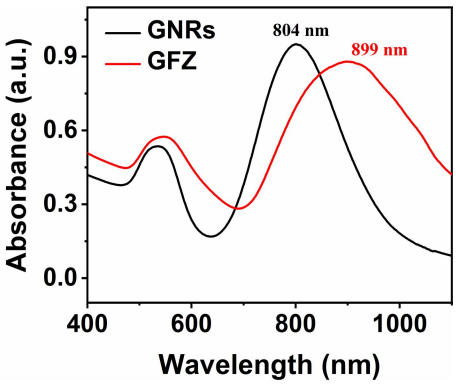

Figure S3. UV−Vis−NIR absorption spectra of GNRs and GFZ.

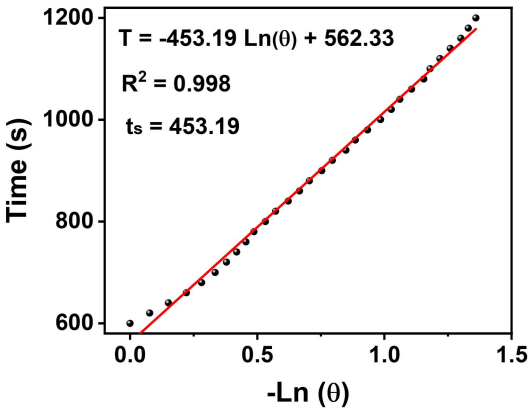

Figure S4. Linear correlation of the cooling times versus negative natural logarithm of driving force temperatures.

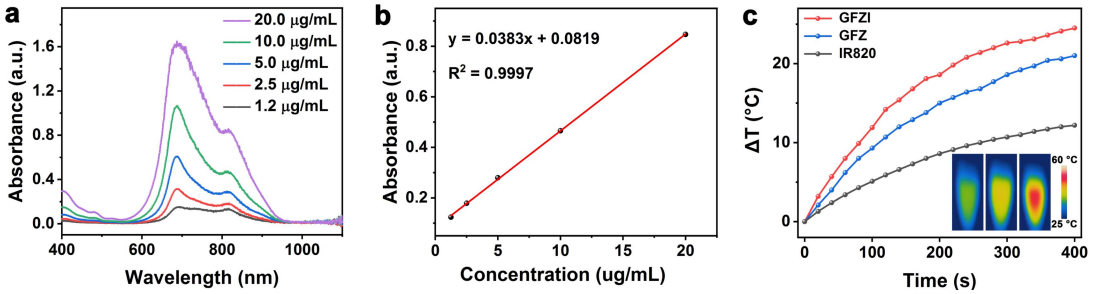

Figure S5. (a) UV-Vis-NIR absorption spectra of IR820 with different concentrations. (b) The standard curve of UV-Vis-NIR absorption spectrum of IR820 (808 nm). (c) The photothermic heating curve of free IR820, GFZ, and GFZI (125 μg/mL) under 808 nm laser irradiation (1 W/cm^2) for 400 s.

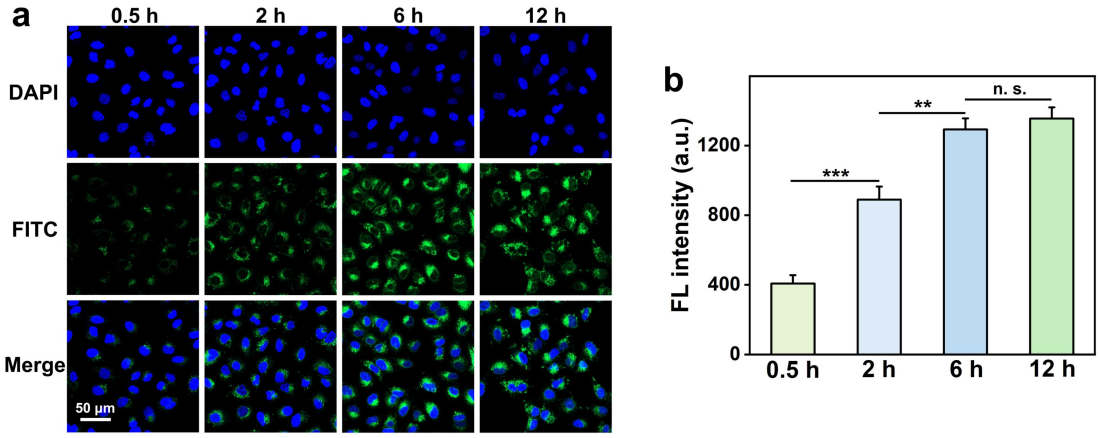

Figure S6. (a) The CLSM images of A549 cells incubated with GFZF at different times and (b) the corresponding quantitative analysis of the fluorescence (FL) intensity. **P < 0.01, ***P < 0.001, n. s.: no significance, n = 3, data represent as mean ± SD.

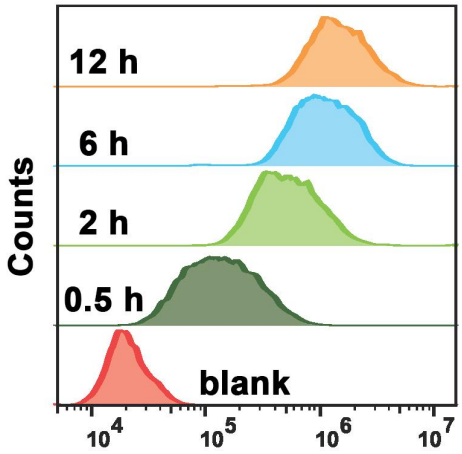

Figure S7. Flow cytometry quantification analysis of A549 cells incubated with the GFZF at different times.

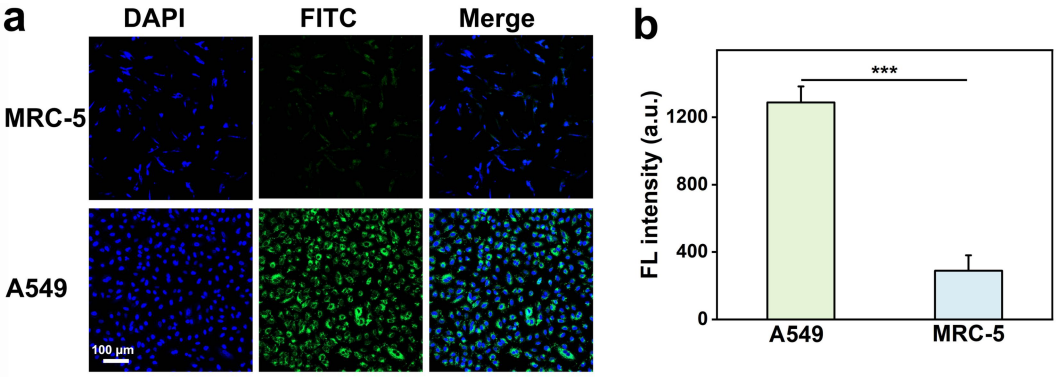

Figure S8. (a) The CLSM images of A549 cells and MRC-5 cells treated with GFZF for 6 h and (b) the corresponding quantitative analysis of the fluorescence intensity. ***P < 0.001, n = 3, data represent as mean ± SD.

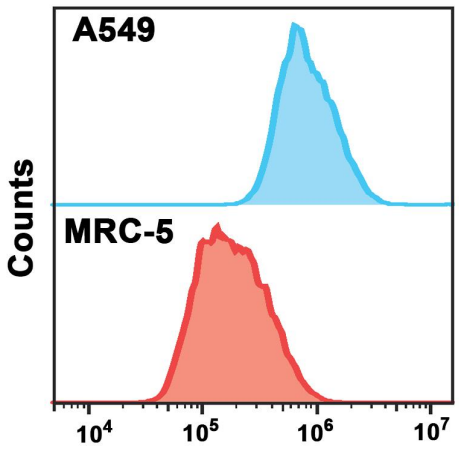

Figure S9. Flow cytometry quantification analysis of A549 cells and MRC-5 cells after incubation with GFZF for 6 h.

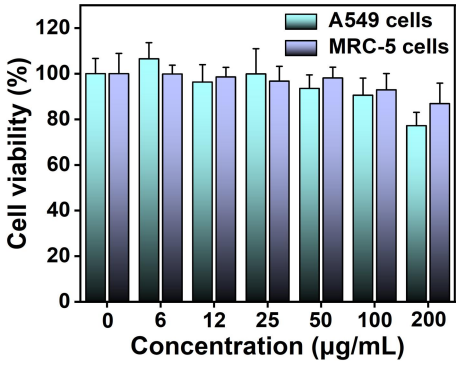

Figure S10. Cell cytotoxicity of GFZI to A549 cells and MRC-5 cells incubated for 24 h.

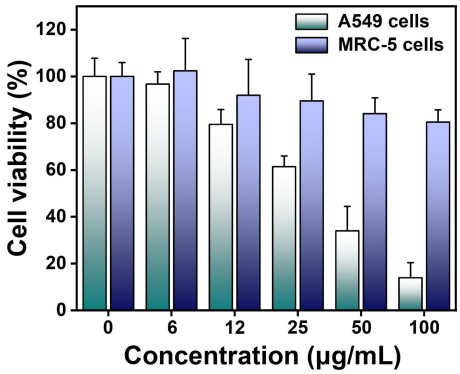

Figure S11. Cell viability of A549 cells and MRC-5 cells treated with GFZI + laser irradiation (808 nm, 1 W/cm^2, 10 min).

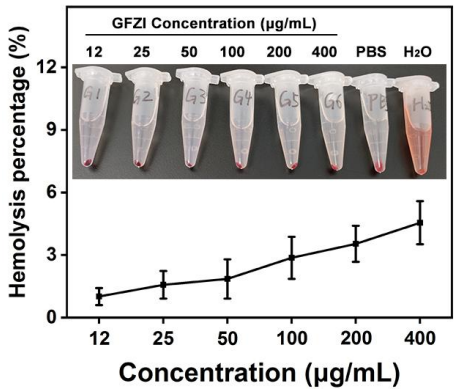

Figure S12. *In vitro* hemolysis percentage of GFZI after incubating with mice RBCs at 37 °C for 2 h at various concentrations. RBCs incubated with PBS and deionized water were used as negative and positive controls, respectively.

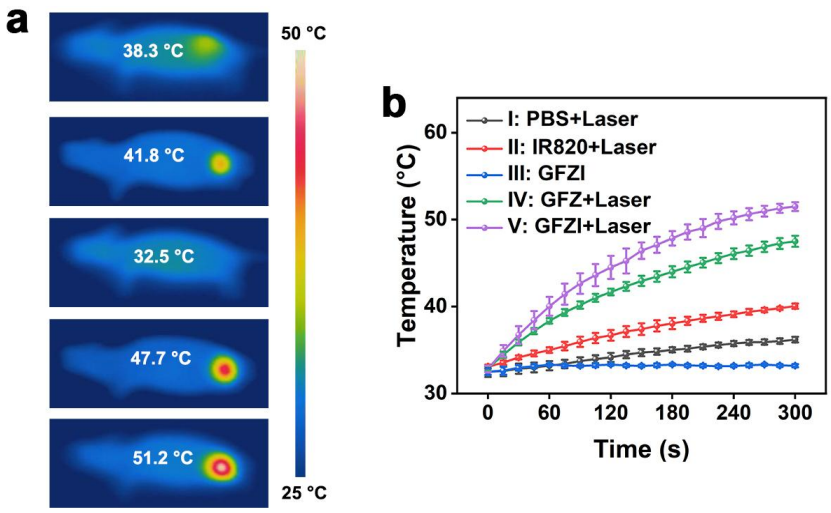

Figure S13. (a) Representative thermal infrared images of mice at 12 h post injected with PBS, IR820, GFZ, or GFZI under 5 min of laser irradiation, respectively. (b) Heating curves of tumor sites with laser irradiation (1 W/cm^2).

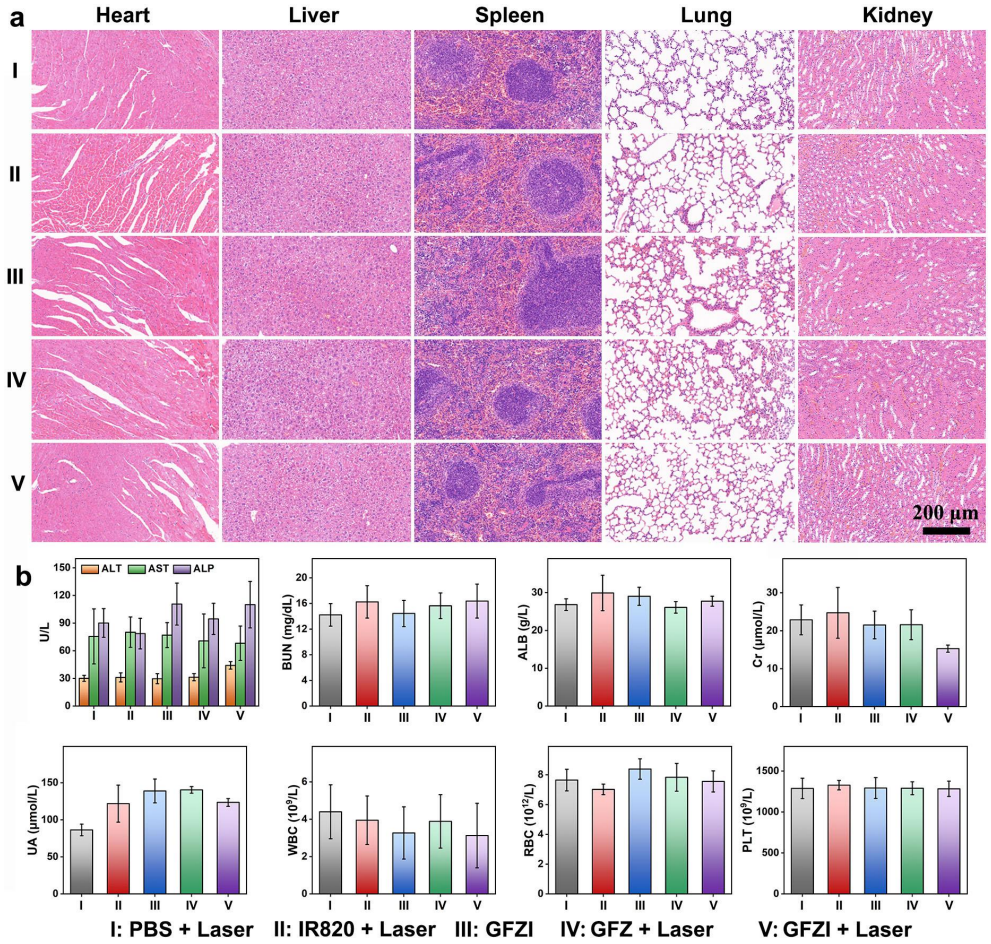

Figure S14. (a) Histological examination of the heart, liver, spleen, lung, and kidney collected from different treatment groups. (b) blood indexes of ALT, AST, ALP, Bun, ALB, Cr, UA, WBC, RBC, and PLT from various groups after 14 d treatment. Data are presented as mean ± SD (n = 3).

References

[1] C. Li, Y. Zhang, Z. Li, E. Mei, J. Lin, F. Li, C. Chen, X. Qing, L. Hou, L. Xiong, H. Hao, Y. Yang, P. Huang, Light-responsive biodegradable nanorattles for cancer theranostics, Adv. Mater. 30(8) (2018) 1706150.

[2] S. Chen, M. Qiu, R. Wang, L. Zhang, C. Li, C. Ye, X. Zhou, Photoactivated nanohybrid for dual-nuclei MR/US/PA multimodal-guided photothermal therapy, Bioconjug. Chem. 33(9) (2022) 1729-1740.

[3] L. Dai, M. Yao, Z. Fu, X. Li, X. Zheng, S. Meng, Z. Yuan, K. Cai, H. Yang, Y. Zhao, Multifunctional metal-organic framework-based nanoreactor for starvation/oxidation improved indoleamine 2,3-dioxygenase-blockade tumor immunotherapy, Nat. Commun. 13(1) (2022) 2688.

[4] Y. Yang, B. Wang, X. Zhang, H. Li, S. Yue, Y. Zhang, Y. Yang, M. Liu, C. Ye, P. Huang, X. Zhou, Activatable graphene quantum-dot-based nanotransformers for long-period tumor imaging and repeated photodynamic therapy, Adv. Mater. 35(23) (2023) e2211337.